Numer. Math. (2007) 108:93–119
DOI 10.1007/s00211-007-0111-0

Numerische Mathematik

Error analysis of finite element approximations of the inverse mean curvature flow arising from the general relativity

Xiaobing Feng · Michael Neilan · Andreas Prohl

Received: 12 September 2006 / Revised: 17 August 2007 / Published online: 21 September 2007

Abstract This paper proposes and analyzes a finite element method for a nonlinear singular elliptic equation arising from the black hole theory in the general relativity. The nonlinear equation, which was derived and analyzed by Huisken and Ilmanen in (J Diff Geom 59:353–437), represents a level set formulation for the inverse mean curvature flow describing the evolution of a hypersurface whose normal velocity equals the reciprocal of its mean curvature. We first propose a finite element method for a regularized flow which involves a small parameter ε; a rigorous analysis is presented to study well-posedness and convergence of the scheme under certain mesh-constraints, and optimal rates of convergence are verified. We then prove uniform convergence of the finite element solution to the unique weak solution of the nonlinear singular elliptic equation as the mesh size h and the regularization parameter ε both tend to zero. Computational results are provided to show the efficiency of the proposed finite element method and to numerically validate the "jumping out" phenomenon of the weak solution of the inverse mean curvature flow. Numerical studies are presented to evidence the existence of a polynomial scaling law between the mesh size h and the regularization parameter ε for optimal convergence of the proposed scheme. Finally, a numerical convergence study for another approach recently proposed by R. Moser (The inverse mean curvature flow and p-harmonic functions. preprint U Bath, 2005) for approximating the inverse mean curvature flow via p-harmonic functions is also included.

X. Feng (✉) · M. Neilan
Department of Mathematics, The University of Tennessee, Knoxville, TN 37996, USA
e-mail: xfeng@math.utk.edu

M. Neilan
e-mail: neilan@math.utk.edu

A. Prohl
Mathematisches Institut, Universität Tübingen, Auf der Morgenstelle 10, 72076 Tübingen, Germany
e-mail: prohl@na.uni-tuebingen.de

Mathematics Subject Classification (2000) 65N30 · 65N12 · 35J70 · 83C57

1 Introduction

The *inverse mean curvature flow* (IMCF) is a one-parameter family of hypersurfaces $\{\Gamma_t\}_{t\geq 0} \subset \mathbf{R}^d$ $(d \geq 2)$ whose normal velocity $V_n(t)$ at each time t equals the inverse of its mean curvature $H(t)$, that is,

$$V_n(t) = \frac{1}{H(t)}. \tag{1}$$

If we let $\Gamma_t := x(\Gamma_0, t)$, then the parametric description of the geometrical law (hence, the inverse mean curvature flow) is to find $x : \Gamma_0 \times [0, T] \to \mathbf{R}^d$ such that

$$\frac{\partial x}{\partial t} = \frac{n}{H} \qquad \forall x \in \Gamma_t, \quad 0 \leq t \leq T, \tag{2}$$

where n denotes the unit outward normal to Γ_t.

The inverse mean curvature flow was originally introduced in [12,20–22] as a mathematical method for proving well-known conjectures from the black hole theory in general relativity such as *Positive Mass Conjecture* (which says that the total mass of any asymptotically flat manifold with nonnegative scalar curvature is nonnegative) (cf. [21,29]), and *Penrose Inequality* (which says that the total mass of a spacetime containing black holes with event horizons of the total area A should be at least $\sqrt{A(16\pi)^{-1}}$, hence, it implies Positive Mass Conjecture) (cf. [2,4,17,22]). It was argued in [22] that the Penrose Inequality would hold if the inverse mean curvature flow would exist for all times and remain smooth, which is generally not expected to be true. In fact, it is known (cf. [19]) that without special geometric assumptions, the mean curvature can tend to zero at some point and singularities develop. When this happens, the classical solution ceases to exist, and it is not clear how to define and/or extend the flow. The problem remained open until the work of Huisken and Ilmanen [17] in 1997. They proposed a level set formulation for the inverse mean curvature flow (1), and defined a weak notion of solutions using an energy minimization principle in such a way that the generalized inverse mean curvature flow exists for all times. Using this generalized flow they then gave the first complete proof of the Penrose Inequality for the case of a single black hole.

It should be noted that the inverse mean curvature flow was also formulated and studied in a general Riemannian manifold (M, g). However, in this paper we only consider the flow in the Euclidean space, i.e., $M = \mathbf{R}^d$, and refer to [17] and the references therein for detailed expositions on the inverse mean curvature flow in a general Riemannian manifold.

Starting with an initial hypersurface Γ_0 satisfying $H(0) \geq 0$, it can be shown that $H(t) \geq 0$ for all $t \geq 0$. Huisken–Ilmanen [17] then propose the following level set formulation for Γ_t

$$\Gamma_t = \partial E_t, \quad E_t := \{x \in \mathbf{R}^d;\ u^0(x) < t\}$$

where the level set function u^0 satisfies the singular elliptic equation

$$\operatorname{div}\left(\frac{\nabla u^0}{|\nabla u^0|}\right) = |\nabla u^0| \tag{3}$$

in the exterior domain $\Omega := \mathbf{R}^d \setminus E_0$ (see Sect. 2 for the precise description of the problem). Note that the left-hand side of (3) describes the mean curvature of the level set Γ_t and the right-hand side yields the inverse speed. We also note that the above level set formulation automatically ensures the mean curvature of the hypersurface is nonnegative as long as a solution exists.

Unlike the situation of the mean curvature flow [6,11,25], the viscosity solution (cf. [5]) of Eq. (3) is not unique. In fact, it is not hard to check that if u is a viscosity solution, so does $\max\{u, s\}$ for any $s \in \mathbf{R}$ (cf. [17]). To select the physically "correct" viscosity solution, Huisken and Ilmanen [17] define a weak solution to Eq. (3) as a locally Lipschitz function u which satisfies

$$J_u(u) \le J_u(v) \tag{4}$$

with

$$J_u(v) := \int_\Omega \left(|\nabla v| + |\nabla u| v \right) dx$$

for every locally Lipschitz function v such that $\{v \neq u\} \subset\subset \Omega$. They proved that such a weak solution is unique and exists for all times (cf. [17,18]), (G. Huisken and T. Ilmanen, High regularities of the inverse mean curvature flow, preprint).

To establish existence and uniqueness of weak solutions, Huisken and Ilmanen regularize the singular/degenerate Eq. (3) to the uniform elliptic equation

$$\operatorname{div}\left(\frac{\nabla u^\varepsilon}{\sqrt{|\nabla u^\varepsilon|^2 + \varepsilon^2}}\right) = \sqrt{|\nabla u^\varepsilon|^2 + \varepsilon^2} \tag{5}$$

for $\varepsilon > 0$ on an appropriately truncated finite domain Ω_L (see Sect. 2 for the precise definition). Smooth solutions to the regularized equation are shown to exist and be unique; then taking the limit as $\varepsilon \to 0$ yields a weak solution u^0 to Eq. (3). As it turns out, the weak solution often has flat regions where u^0 equals a constant. Hence, the t-level sets Γ_t of u^0 are discontinuous in t, which corresponds to the "jumping out" phenomenon of the weak solution of the inverse mean curvature flow (cf. [17]). In addition, due to the singular nature of Eq. (3), numerically it is not feasible to compute its solution without a regularization. Our earlier experience with another singular problem of the same type, the total variation flow [13,14], suggests that the regularization (5) can also be utilized to develop practical numerical methods for approximating the solution of Eq. (3).

The goal of this paper is to construct and analyze a finite element method for approximating the solution of Eq. (5) for each $\varepsilon > 0$ and for approximating the solution of

Eq. (3) via Eq. (5) by taking $\varepsilon \to 0$. If compared with the total variation flow equation considered in [13,14], the new nonlinear term on the right-hand side of (5) poses an additional difficulty for error estimates for any numerical approximation of equation (5), because the error due to this term in the error equation is too strong to be completely absorbed by the positive term contributed by the term on the left-hand side. The error equation in fact resembles a typical error equation of a non-coercive problem [10,31] although Eq. (5) is uniformly elliptic. To the best of our knowledge, the only numerical result that appears in the literature for the inverse mean curvature flow is the work of Pasch [26], which proposed some finite volume method for approximating the regularized equation (5) with Neumann boundary condition on outer boundary of the truncated domain Ω_L. Pasch also provides three-dimensional numerical simulations for the inverse mean curvature flow; however, no rigorous convergence analysis is known for the proposed finite volume method.

The rest of the paper is organized as follows. In Sect. 2 we first give precise descriptions of the boundary value problem (3) and (5), respectively. We then recall some theoretical results proved in [17] for both problems. We conclude Sect. 2 with a brief derivation of the linearization (at the solution) of the differential operator in (5) and its properties, which will play an important role for the error analysis in Sect. 3. In Sect. 3 we propose a finite element method for approximating equation (5), address its well-posedness, and derive optimal order error estimates in $W^{1,p}$-norm for the finite element method provided a mesh-constraint $F(\varepsilon, h) \geq 0$ and smallness of the mesh-size $h > 0$ hold. Our main ideas are to adapt a fixed point argument of [27] (also see [16]) for general nonlinear problems, and to make strong use of the stability property of the linearized (weakly coercive) problem and its finite element approximations. Carrying out each of these ideas requires some mesh-constraint to hold (cf. Sect. 3.1 for the details). In addition, optimal error estimates in L^p-norm are also derived using a duality argument. In Sect. 4 we show that the finite element solution converges uniformly to the weak solution of the original nonlinear singular equation (3) as the regularization parameter ε tends to zero, provided that a mesh-constraint $F(\varepsilon, h) \geq 0$ holds. Finally, in Sect. 5 we first present some computational results to show the efficiency of the proposed finite element method and to numerically validate the "jumping out" phenomenon of the weak solution of the inverse mean curvature flow as predicted and proved by Huisken and Ilmanen in [17].

We then give a numerical study for determining the "best" choice of mesh size $h = h(\varepsilon)$, and numerically estimate rates of convergence for both $u^0 - u_h^\varepsilon$ and $u^0 - u^\varepsilon$, all in terms of powers of ε. Finally, we include a numerical study of the rates of convergence for a new approach proposed by R. Moser (The inverse mean curvature flow and p-harmonic functions. preprint U Bath, 2005) for approximating the inverse mean curvature flow via p-harmonic functions (see Remark 3).

2 Description of problems and preliminaries

Standard space and norm notations are adopted in this paper, for example, $W^{m,p}(\Omega)$ denotes the Sobolev space of functions whose up to mth order derivatives are L^p-integrable, $W^{0,p}(\Omega) := L^p(\Omega)$, and $\|\cdot\|_{W^{m,p}} = \|\cdot\|_{W^{m,p}(\Omega)}$. $(\cdot,\cdot)$ denotes the

standard L^2-inner product, and $\langle \cdot, \cdot \rangle$ denotes the dual product between a Banach space X and its dual space X'. We refer to [1,15,23] for the precise definitions of these spaces and their norms. In addition, we introduce the following special notation

$$|\, z \,|_\varepsilon = f_\varepsilon(z) := \sqrt{|z|^2 + \varepsilon^2} \quad \forall z \in \mathbf{R}^d. \tag{6}$$

Throughout this paper, C denotes a generic constant which is independent of ε and the solutions of Eqs. (3) and (5).

For an initial hypersurface $\Gamma_0 \subset \mathbf{R}^d$ with nonnegative mean curvature $H(0, x) \geq 0$ for all $x \in \Gamma_0$, it is easy to see that $H(t, x)$ of the inverse mean curvature flow (1) remains nonnegative as long as the flow exists. In other words, the flow Γ_t only moves in one direction and expands in time. To exploit this causality of the inverse mean curvature flow, in Huisken–Ilmanen [17] propose to represent the flow as the t level set of a function u^0 which is defined in $\mathbf{R}^d$ and takes zero value on the initial hypersurface Γ_0. That is, for $t \geq 0$

$$\Gamma_t := \{x \in \mathbf{R}^d;\ u^0(x) = t\} = \partial E_t, \quad E_t := \{x \in \mathbf{R}^d;\ u^0(x) < t\}. \tag{7}$$

Physically, one can interpret $t = u^0(x)$ as the *first arrival time* of the flow at x. Note that the causality of the inverse mean curvature flow guarantees that the flow visits every x outside of the initial hypersurface Γ_0 only once, hence, u^0 is a single-valued function.

Differentiating the equation $t = u^0(x)$ with respect to t (note that x is a function of t), using the chain rule and the fact that

$$H(t, x) = \operatorname{div}\left(\frac{\nabla u^0}{|\nabla u^0|}\right),$$

it is easy to check that if (7) is true, then the inverse mean curvature flow (1) reduces to Eq. (3) for u^0. Precisely, the level set function u^0 must satisfy the following boundary value problem [18]

$$\operatorname{div}\left(\frac{\nabla u^0}{|\nabla u^0|}\right) = |\nabla u^0| \quad \text{in } \Omega := \mathbf{R}^d \setminus E_0, \tag{8}$$

$$u^0 = 0 \quad \text{on } \Gamma_0, \tag{9}$$

$$u^0 \to \infty \quad \text{as } |x| \to \infty. \tag{10}$$

Remark 1 The differential operator on the left-hand side of Eq. (8) is a *singular* elliptic operator. Formally, it may be regarded as 1-Laplacian since it corresponds to the p-Laplacian $\operatorname{div}(|\nabla u^0|^{p-2}\nabla u^0)$ with $p = 1$. Also formally, it can be obtained as the Euler–Lagrange operator for the least gradient functional, and more generally for the total variation functional

$$\mathcal{J}(u) := \int_\Omega |\nabla u|\, dx.$$

We remark that the 1-Laplacian plays a very important role in the Variational PDE Method for image processing, see [13,14,24] and the references therein.

Due to the success of using the viscosity solution method to analyze the (level set) mean curvature flow [6,11], it is natural to use the method to analyze the (level set) inverse mean curvature flow (8)–(10). It turns out that there are some big differences between the mean curvature flow and the inverse mean curvature flow (see [17] for more discussions). As pointed out in Sect. 1, one of the differences, observed by Huisken and Ilmanen [17], is that unlike the level set equation for the mean curvature flow, the viscosity solution of (8)–(10) is *not* unique. In fact, if u^0 is a viscosity solution, so does $\min\{u^0, s\}$ for any $s \in \mathbf{R}$. Hence, a selection criterion must be specified in order to single out the physically "correct" solution. It turns out that the variation equation (4) provides such a criterion.

Theorem 1 (Theorem 3.1 of [17], also see [18]) *The boundary value problem* (8)–(10) *has a unique* (*Lipschitz continuous*) *viscosity solution* u^0 *satisfying* (4). *Moreover,*

$$|\nabla u^0(x)| \leq \sup_{y \in B_r(x) \cap \Gamma_0} |H(0, y)| + \frac{C(d)}{r} \qquad a.e.\ x \in \Omega, \tag{11}$$

for each $0 < r < \infty$.

As pointed out in Sect. 1, to prove Theorem 1, Huisken and Ilmanen approximated equation (8) by the regularized equation (5), which is considered on a truncated domain. More precisely, the regularized boundary value problem is defined as

$$\operatorname{div}\left(\frac{\nabla u^\varepsilon}{|\nabla u^\varepsilon|_\varepsilon}\right) = |\nabla u^\varepsilon|_\varepsilon \qquad \text{in } \Omega_L \subset \Omega, \tag{12}$$

$$u^\varepsilon = 0 \qquad \text{on } \Gamma_0, \tag{13}$$

$$u^\varepsilon = L \qquad \text{on } \partial\Omega_L^+. \tag{14}$$

Here $\Omega_L := B_{\frac{1}{\varepsilon}}(0) \cap \Omega$ and L is a (large) positive constant. $\partial\Omega_L^+$ denotes the outer boundary of Ω_L.

For problem (12)–(14), Huisken and Ilmanen proved the following result (cf. Lemma 3.5 of [17]).

Theorem 2 *For every* $L > 0$, *there exists* $\varepsilon(L) > 0$, *such that the boundary value problem* (12)–(14) *has a unique smooth solution for all* $0 < \varepsilon < \varepsilon(L)$.

Remark 2 (a) The proof is based on the study of the auxiliary problem for $u^{\varepsilon,\tau}$: $\Omega_L \to \mathbf{R}$ to satisfy (12)–(13), and $u^{\varepsilon,\tau}\Big|_{\partial\Omega_L^+} = \tau$, for $0 \leq \tau \leq L - 2$: solvability for the case $\tau = 0$, and $\varepsilon \geq 0$ sufficiently small follows from implicit function theorem. The method of continuity is then applied to extend this result to $0 \leq \tau \leq L - 2$.

(b) The solution u^ε also satisfies a number of other properties such as the Maximum Principle. See Lemma 3.4 of [17].

(c) In general, the precise dependence of $\varepsilon(L)$ on L is complicated. On the other hand, it is known that $\varepsilon(L)$ tends to zero as L tends to infinity. It should be noted that for a given $\varepsilon > 0$, if L is too large, the boundary value problem (12)–(14) may have no solution! See Example 3.2 of [17]. Indeed, our numerical experiments in Sect. 5 also verify this fact.

(d) It is easy to check that the solution of (12)–(14) satisfies the variational equation

$$\int_{\Omega_L} \left\{ \frac{\nabla u^\varepsilon \cdot \nabla v}{|\nabla u^\varepsilon|_\varepsilon} + |\nabla u^\varepsilon|_\varepsilon \, v \right\} dx = 0 \qquad \forall v \in W_0^{1,2}(\Omega_L). \tag{15}$$

The above variational equation will serve as the starting point for us to construct finite element methods in Sect. 3.

By passing to the limit as $\varepsilon \to 0$, hence, $L \to \infty$, Huisken and Ilmanen were able to prove the existence result stated in Theorem 1. Specifically,

Theorem 3 *For $\varepsilon > 0$, let u^ε denote the solution of (12)–(14), then there exists a Lipschitz function u^0 such that*

$$\lim_{\varepsilon \to 0} \| u^0 - u^\varepsilon \|_{L^\infty_{loc}} = 0, \tag{16}$$

and u^0 is a viscosity solution of (8)–(10) satisfying (4).

Proof See the proof of Theorem 3.1 on pp. 389–390 of [17]. □

Remark 3 Recently Moser (The inverse mean curvature flow and p-harmonic functions. preprint U Bath, 2005) constructed proper weak solutions for problem (8)–(10) using an alternative approach which links problem (8)–(10) to the theory of p-harmonic functions. Specifically, he proved

$$(1-p)\log v^{(p)} \longrightarrow u^0 \qquad \text{as } p \to 1^+$$

locally uniformly in $\overline{\Omega}$, where $v^{(p)}$ solves

$$-\text{div}\left(|\nabla v^{(p)}|^{p-2}\nabla v^{(p)}\right) = 0 \quad \text{in } \Omega\,, \qquad v^{(p)} = 1 \quad \text{on } \partial\Omega \tag{17}$$

for $p > 1$. The regularity $u^0 \in C^{0,1}_{loc}(\overline{\Omega})$ then follow from the theory of p-harmonic functions.

In Sect. 5.2, we shall provide some numerical experiments for Moser's approach. In particular, we shall numerically analyze its rate of convergence in terms of powers of $(p-1)$.

We conclude this section by studying the linearization (at the solution u^ε) of the nonlinear differential operator that results from Eq. (12). The property of this linearization will play an important role for our error analysis in the next section.

Let $\mathcal{M}_\varepsilon : W^{1,2}(\Omega_L) \to W^{-1,2}(\Omega_L)$ denote this differential operator, that is,

$$\mathcal{M}_\varepsilon(v) := -\mathrm{div}\left(\frac{\nabla v}{|\nabla v|_\varepsilon}\right) + |\nabla v|_\varepsilon. \tag{18}$$

The linearization of $\mathcal{M}_\varepsilon$ at the solution of (12)–(14) is defined by

$$\mathcal{L}_{u^\varepsilon}(\varphi) := -\mathrm{div}\left(D^2 f_\varepsilon(\nabla u^\varepsilon)\nabla\varphi\right) + Df_\varepsilon(\nabla u^\varepsilon)\cdot\nabla\varphi, \tag{19}$$

where $Df_\varepsilon(z)$ and $D^2 f_\varepsilon(z)$ denote the gradient and the Hessian of $f_\varepsilon(z)$ with respect to z, that is

$$Df_\varepsilon(z) = \frac{z}{|z|_\varepsilon}, \qquad D^2 f_\varepsilon(z) = \frac{|z|_\varepsilon^2 I - z^t z}{|z|_\varepsilon^3} \qquad \forall z \in \mathbf{R}^d, \tag{20}$$

where I stands for $d \times d$ identity matrix and z^t denotes the transpose of z.

Since

$$D^2 f_\varepsilon(z)\xi\cdot\xi = \frac{\varepsilon^2|\xi|^2 + \left(|\xi|^2|z|^2 - |z\cdot\xi|^2\right)}{|z|_\varepsilon^3} \geq \frac{\varepsilon^2|\xi|^2}{|z|_\varepsilon^3} \quad \forall \xi \in \mathbf{R}^d, \tag{21}$$

then $\mathcal{L}_{u^\varepsilon}$ is elliptic for $\varepsilon \geq 0$, and *uniformly* elliptic for $\varepsilon > 0$. So is $\mathcal{L}^*_{u^\varepsilon}$, the adjoint operator of $\mathcal{L}_{u^\varepsilon}$ with respect to L^2-inner product, that is,

$$\mathcal{L}^*_{u^\varepsilon}(\varphi) = -\mathrm{div}\left(D^2 f_\varepsilon(\nabla u^\varepsilon)\nabla\varphi + Df_\varepsilon(\nabla u^\varepsilon)\,\varphi\right). \tag{22}$$

It is easy to check that there holds the following Gårding's inequality

$$\langle\mathcal{L}_{u^\varepsilon}(\varphi), \varphi\rangle \geq c_0\,\varepsilon^2\,\|\nabla\varphi\|^2_{L^2} - d\varepsilon^{-2}\|\varphi\|^2_{L^2} \quad \forall\varphi \in W^{1,2}_0(\Omega_L), \tag{23}$$

for some positive constant c_0 independent of ε (see p. 389 of [17]).

Since u^ε is smooth (cf. Theorem 2), from the standard theory for uniformly elliptic equations (cf. [15,23,28]) we have

Lemma 1 *Let $\partial\Omega_L \in C^{k+2}$, $k \geq -1$ and $1 < p < \infty$, for any $g \in W^{k,p}(\Omega_L)$ and $\phi \in W^{k+2,p}(\Omega_L)$, the boundary value problem*

$$\mathcal{L}(\varphi) = g \quad \text{in } \Omega_L, \tag{24}$$

$$\varphi = \phi \quad \text{on } \partial\Omega_L, \tag{25}$$

has a unique solution $\varphi \in W^{k+2,p}(\Omega_L)$, for $\mathcal{L} = \mathcal{L}_{u^\varepsilon}$, or $\mathcal{L}^*_{u^\varepsilon}$. Moreover, there exists a positive constant $C_0 = C_0(\varepsilon)$, such that

$$\|\varphi\|_{W^{k+2,p}} \leq C_0\left(\|g\|_{W^{k,p}} + \|\phi\|_{W^{k+2,p}}\right). \tag{26}$$

Remark 4 To trace the explicit dependence of $C_0 = C_0(\varepsilon)$ on ε^{-1} requires sharp bounds for the solution of (12)–(14) in terms of ε^{-1} in higher norms, which is a non-trivial task (G. Huisken, personal commmunication); in fact, asymptotical behavior of constants $C_j = C_j(\varepsilon)$, $1 \le j \le 8$ for $\varepsilon \to 0$ used below could be specified once the asymptotics of $\varepsilon \mapsto C_0(\varepsilon)$ would be available. A large part of Sect. 5 is devoted to numerically address this issue.

3 Finite element approximations

3.1 Formulation, well-posedness, and error estimates in energy norm

Let $\mathcal{T}_h$ be a quasi-uniform triangulation of Ω_L ($K \in \mathcal{T}_h$ are tetrahedrons when $d = 3$) with mesh size $h \in (0, 1)$. Let V_r^h denote the finite element space of continuous, rth order piecewise polynomials associated with $\mathcal{T}_h$, that is, for $r \ge 1$

$$
\begin{aligned}
V_r^h &:= \left\{ v_h \in C^0(\overline{\Omega}_L);\ \ v_h|_K \in P_r(K),\ \ \forall K \in \mathcal{T}_h \right\} \subset W^{1,2}(\Omega_L),\\
V_r^{h,b} &:= \left\{ v_h \in V_r^h;\ \ v_h = I_h^r u^\varepsilon \text{ on } \partial\Omega_L \right\},\\
V_r^{h,0} &:= V_r^h \cap W_0^{1,2}(\Omega_L),
\end{aligned}
$$

where $I_h^r : C^0(\overline{\Omega}_L) \to V_r^h$ denotes the standard Lagrange interpolation operator. Based on the variational equation (15), our finite element method for (12)–(14) is defined as seeking $u_h^\varepsilon \in V_r^{h,b}$ such that

$$
\int_{\Omega_L} \left\{ \frac{\nabla u_h^\varepsilon \cdot \nabla v_h}{|\nabla u_h^\varepsilon|_\varepsilon} + |\nabla u_h^\varepsilon|_\varepsilon\, v_h \right\} dx = 0 \qquad \forall v_h \in V_r^{h,0}. \tag{27}
$$

To address the solvability of scheme (27), we first need to analyze the solvability and stability for the finite element approximation of (24), (25) with $\mathcal{L} = \mathcal{L}_{u^\varepsilon}$ and $\phi = I_h^r u^\varepsilon$. The subsequent assertion evidences small, restricted choices $h_0 = h_0(\varepsilon)$ for this purpose.

Lemma 2 *Let $\varphi \in W^{2+k,p}(\Omega_L)$ denote the unique solution of (24), (25) with $\mathcal{L} = \mathcal{L}_{u^\varepsilon}$, and $h_0 = O(\varepsilon^3 C_0^{-1})$. Then, for all $h \le h_0$, there exists a unique solution $\varphi_h \in V_r^{h,b}$ to the problem*

$$
\langle \mathcal{L}_{u^\varepsilon}(\varphi_h), v_h \rangle = \langle g, v_h \rangle \qquad \forall\, v_h \in V_r^{h,0}. \tag{28}
$$

Moreover, for $1 < p < \infty$

$$
\|\varphi - \varphi_h\|_{L^2} + h\|\nabla(\varphi - \varphi_h)\|_{L^2} \le C_1 h^{r+1} \left(\|g\|_{W^{r-1,2}} + \|\phi\|_{W^{r+1,2}} \right), \tag{29}
$$

$$
\|\varphi_h\|_{W^{1,p}} \le C_2 \left(\|g\|_{W^{-1,p}} + \|\phi\|_{W^{1,p}} \right), \tag{30}
$$

$$
\|\varphi - \varphi_h\|_{W^{1,p}} \le C_3\, h^r \left(\|g\|_{W^{r-1,p}} + \|\phi\|_{W^{r+1,p}} \right), \tag{31}
$$

where $C_j = C_j(\varepsilon)$ are some positive constants which depend on ε^{-1}.

Proof The existence and uniqueness, as well as estimate (29) follow immediately from (26), (20), (23), and an application of [3, Theorem 5.7.6], whose proof is known as the Schatz argument [31].

The Assertions (30) and (31) follow from appealing to the general results of [3, Theorem 7.5.3] and using (26). □

Next, for a given $w_h \in V_r^{h,b}$, we define $T(w_h) \in V_r^{h,b}$ by

$$\langle \mathcal{L}_{u^\varepsilon}(w_h - T(w_h)), \psi_h \rangle = \left(\frac{\nabla w_h}{|\nabla w_h|_\varepsilon}, \nabla \psi_h \right) + (|\nabla w_h|_\varepsilon, \psi_h) \tag{32}$$

for all $\psi_h \in V_r^{h,0}$. Clearly, T is a mapping from $V_r^{h,b}$ into itself, and from Lemma 2 we conclude that $T(w_h)$ is well defined and one-to-one if $h \le h_0$.

We note that the right-hand side of (32) is the left-hand side of (27) with (w_h, ψ_h) in the place of (u_h^ε, v_h), and it is trivial to see that any fixed point u_h of the mapping T (i.e., $u_h = T(u_h)$) is a solution of problem (27). In the following we shall show that the mapping T has a unique fixed point, hence problem (27) has a unique solution, in a small neighborhood of $I_h^r u^\varepsilon$. To this end, we define

$$B_{p,h}(\rho) = B_p(I_h^r u^\varepsilon, \rho) := \{ v_h \in V_r^{h,b} : \| v_h - I_h^r u^\varepsilon \|_{W^{1,p}} \le \rho \},$$

then we have

Lemma 3 *There exist a positive constant $C_4 = C_4(\varepsilon)$, and a sufficiently small number $h_1 > 0$ such that for $h \le \min\{h_0, h_1\}$ there holds*

$$\| I_h^r u^\varepsilon - T(I_h^r u^\varepsilon) \|_{W^{1,p}} \le C_4 h^r \| u^\varepsilon \|_{W^{r+1,p}} \quad \forall\, 1 < p < \infty. \tag{33}$$

Proof From the definition of $T(I_h^r u^\varepsilon)$ we conclude that $I_h^r u^\varepsilon - T(I_h^r u^\varepsilon)$ is the unique solution of (28) with zero boundary value and

$$g = -\mathrm{div}\left(\frac{\nabla I_h^r u^\varepsilon}{|\nabla I_h^r u^\varepsilon|_\varepsilon} \right) + |\nabla I_h^r u^\varepsilon|_\varepsilon,$$

provided that $h \le h_0$. It then follows from (30) that

$$\| I_h^r u^\varepsilon - T(I_h^r u^\varepsilon) \|_{W^{1,p}} \le C_2 \| g \|_{W^{-1,p}}. \tag{34}$$

Now, let p' be the conjugate number of p, P_h denote the L^2-projection operator onto $V_r^{h,b}$, and $\eta_h^\varepsilon = I_h^r u^\varepsilon - u^\varepsilon$. Using (15) and Schwarz inequality we get for $\psi_h = P_h \psi$ with $\psi \in W^{1,p'}(\Omega_L)$ that

$$\begin{aligned} \langle g, \psi_h \rangle &= \left(\frac{\nabla I_h^r u^\varepsilon}{|\nabla I_h^r u^\varepsilon|_\varepsilon} - \frac{\nabla u^\varepsilon}{|\nabla u^\varepsilon|_\varepsilon}, \nabla \psi_h \right) + \left(|\nabla I_h^r u^\varepsilon|_\varepsilon - |\nabla u^\varepsilon|_\varepsilon, \psi_h \right) \\ &= \left(A_h^\varepsilon \nabla \eta_h^\varepsilon, \nabla \psi_h \right) + \left(a_h^\varepsilon \cdot \nabla \eta_h^\varepsilon, \psi_h \right), \end{aligned}$$

where

$$A_h^\varepsilon := \int_0^1 D^2 f_\varepsilon \left(\nabla u^\varepsilon + t\nabla(I_h^r u^\varepsilon - u^\varepsilon)\right)\, dt,$$

$$a_h^\varepsilon := \int_0^1 Df_\varepsilon \left(\nabla u^\varepsilon + t\nabla(I_h^r u^\varepsilon - u^\varepsilon)\right)\, dt.$$

Since

$$\left|(A_h^\varepsilon)_{ij}\right| \le 2\varepsilon^{-1}, \quad \left|(a_h^\varepsilon)_i\right| \le 1 \quad \text{for } 1 \le i, j \le d,$$

and the $W^{1,p'}$-continuity of the projection operator P_h (cf. [8]), there exists a sufficiently small number $h_1 = h_1(\varepsilon) > 0$ such that for $h \le h_1$

$$\begin{aligned} \| g \|_{W^{-1,p}} &\le 2 \sup_{\substack{\psi \in W^{1,p'}(\Omega_L) \\ \| \psi \|_{W^{1,p'}} \le 1}} |\langle g, \psi \rangle| \\ &\le 6\varepsilon^{-1} \| \nabla \eta_h^\varepsilon \|_{L^p} \le C\, \varepsilon^{-1} h^r \| u^\varepsilon \|_{W^{r+1,p}}. \end{aligned} \tag{35}$$

The proof is complete after setting $C_4 = C_2 C \varepsilon^{-1}$. □

Next lemma establishes a contracting property of the mapping T.

Lemma 4 *Let h_0 and h_1 be same as in Lemma 3. Then, there exists another small number $h_2 > 0$ such that for $h \le \min\{h_0, h_1, h_2\}$, let $\rho_0 = \frac{1}{144} C_2^{-1} h^{\frac{d}{p}} \varepsilon^2$, the mapping T is a contracting mapping in the ball $B_{p,h}(\rho_0)$ with the contraction factor $\frac{1}{2}$, that is, for any $v_h, w_h \in B_{p,h}(\rho_0)$*

$$\| T(v_h) - T(w_h) \|_{W^{1,p}} \le \frac{1}{2} \| v_h - w_h \|_{W^{1,p}} \quad \forall\, p \in \left(\frac{d}{r}, \infty\right). \tag{36}$$

Proof For any $v_h, w_h \in B_{p,h}(\rho_0)$, let $\xi_h = v_h - w_h$, subtracting the two copies of Eq. (32) which define $T(v_h)$ and $T(w_h)$ and using the Mean Value Theorem of integration yield that for any $\psi_h \in V_r^{h,0}$

$$\begin{aligned} \langle \mathcal{L}_{u^\varepsilon}(T(v_h) - T(w_h)), \psi_h \rangle = &\left([D^2 f_\varepsilon(\nabla u^\varepsilon) - A_h^\varepsilon] \nabla \xi_h, \nabla \psi_h \right) \\ &+ \left([Df_\varepsilon(\nabla u^\varepsilon) - a_h^\varepsilon] \cdot \nabla \xi_h, \psi_h \right), \end{aligned} \tag{37}$$

where

$$A_h^\varepsilon := \int_0^1 D^2 f_\varepsilon \left(\nabla w_h + t\nabla(v_h - w_h)\right) dt,$$

$$a_h^\varepsilon := \int_0^1 Df_\varepsilon \left(\nabla w_h + t\nabla(v_h - w_h)\right) dt.$$

Note that we have abused the notation by using A_h^ε and a_h^ε to denote different expressions in different proofs.

For $h \le h_0$, (37) implies that $T(v_h) - T(w_h)$ is the unique solution to (28) with zero boundary value and

$$g = -\mathrm{div}\left([D^2 f_\varepsilon(\nabla u^\varepsilon) - A_h]\nabla\xi_h\right) + [Df_\varepsilon(\nabla u^\varepsilon) - a_h]\cdot\nabla\xi_h.$$

Then, it follows from (30) that

$$\| T(v_h) - T(w_h) \|_{W^{1,p}} \le C_2 \| g \|_{W^{-1,p}}. \tag{38}$$

From

$$\frac{\partial}{\partial z_k}(D^2 f_\varepsilon(z))_{ij} = -\frac{z_k\delta_{ij} + z_j\delta_{ik} + z_i\delta_{jk}}{|z|_\varepsilon^3} + \frac{3z_i z_j z_k}{|z|_\varepsilon^5}, \tag{39}$$

and the Mean Value Theorem we get

$$\begin{aligned}
&\left|D^2 f_\varepsilon(\nabla u^\varepsilon) - A_h^\varepsilon\right| \le 9\varepsilon^{-2}\left(|\nabla(u^\varepsilon - v_h)| + |\nabla(u^\varepsilon - w_h)|\right)\\
&\quad \le 18\varepsilon^{-2}\left(|\nabla(u^\varepsilon - I_h^r u^\varepsilon)| + |\nabla(I_h^r u^\varepsilon - v_h)| + |\nabla(I_h^r u^\varepsilon - w_h)|\right),\\
&\left|Df_\varepsilon(\nabla u^\varepsilon) - a_h^\varepsilon\right| \le 2\varepsilon^{-1}\left(|\nabla(u^\varepsilon - v_h)| + |\nabla(u^\varepsilon - w_h)|\right)\\
&\quad \le 4\varepsilon^{-1}\left(|\nabla(u^\varepsilon - I_h^r u^\varepsilon)| + |\nabla(I_h^r u^\varepsilon - v_h)| + |\nabla(I_h^r u^\varepsilon - w_h)|\right),
\end{aligned}$$

which together with the Schwarz inequality and an inverse inequality imply for $\psi_h = P_h\psi$ with $\psi \in W^{1,p'}(\Omega_L)$ that

$$\begin{aligned}
|\langle g, \psi_h\rangle| &\le 9\varepsilon^{-2}\Big\{\| \nabla(u^\varepsilon - v_h)\|_{L^\infty} + \| \nabla(u^\varepsilon - w_h)\|_{L^\infty}\\
&\qquad + \varepsilon^{-1}\left(\| \nabla(u^\varepsilon - v_h)\|_{L^\infty} + \| \nabla(u^\varepsilon - w_h)\|_{L^\infty}\right)\Big\} \| \nabla\xi_h\|_{L^p} \| \psi_h\|_{L^{p'}}\\
&\le 72\varepsilon^{-2}\left(h^r + \rho_0 h^{-\frac{d}{p}}\right) \| \nabla\xi_h\|_{L^p} \| \nabla\psi_h\|_{L^{p'}}.
\end{aligned}$$

Hence, as above, there exists a small number $h_2 = h_2(\varepsilon)$ such that for $h \le h_2$

$$\| g \|_{W^{-1,p}} \le 72\varepsilon^{-2}\left(h^r + \rho_0 h^{-\frac{d}{p}}\right) \| \nabla\xi_h\|_{L^p}. \tag{40}$$

It follows from (38), (40), and the definition of ρ_0 that

$$\begin{aligned}\| T(v_h) - T(w_h) \|_{W^{1,p}} &\le 72 C_2 \varepsilon^{-2} \left(h^r + \rho_0 h^{-\frac{d}{p}} \right) \| v_h - w_h \|_{W^{1,p}} \\ &\le \frac{1}{2} \| v_h - w_h \|_{W^{1,p}}.\end{aligned}$$

The proof is complete. □

Remark 5 The reason for restricting $p > \frac{d}{r}$ is to ensure that T maps the center $I_h^r u^\varepsilon$ of the ball $B_{p,h}(\rho_0)$ into the ball, this fact will be used in the proof of the next theorem.

We are now ready to state the first main theorem of this paper.

Theorem 4 *Let u^ε denote the unique solution to problem (12)–(14) (cf. Theorem 2), h_0, h_1 and h_2 be same as in Lemma 4. For $h \le \min\{h_0, h_1, h_2\}$, let $\rho_1 = 2C_4 h^r$, then the finite element method (27) has a unique solution u_h^ε in the ball $B_{p,h}(\rho_1)$ for $p > \frac{d}{r}$. Moreover, there exists $C_5 = C_5(\varepsilon)$, such that*

$$\| u^\varepsilon - u_h^\varepsilon \|_{W^{1,p}} \le C_5 h^r \| u^\varepsilon \|_{W^{r+1,p}} \qquad \forall r \ge 1,\ p > \frac{d}{r}. \tag{41}$$

Proof Since $B_{p,h}(\rho_1) \subset B_{p,h}(\rho_0)$, Lemma 4 implies that the mapping T is also a contracting mapping in $B_{p,h}(\rho_1)$ with the contraction factor $\frac{1}{2}$. We shall show that T also maps $B_{p,h}(\rho_1)$ into itself.

For any $v_h \in B_{p,h}(\rho_1)$, it follows from Lemma 3, Lemma 4, and the triangle inequality that

$$\begin{aligned}&\| I_h^r u^\varepsilon - T(v_h) \|_{W^{1,p}} \\ &\quad \le \| I_h^r u^\varepsilon - T(I_h^r u^\varepsilon) \|_{W^{1,p}} + \| T(I_h^r u^\varepsilon) - T(v_h) \|_{W^{1,p}} \\ &\quad \le C_4 h^r + \frac{1}{2} \| I_h^r u^\varepsilon - v_h \|_{W^{1,p}} \le \frac{\rho_1}{2} + \frac{\rho_1}{2} = \rho_1.\end{aligned} \tag{42}$$

Hence, $T(v_h) \in B_{p,h}(\rho_1)$. Consequently, T has a unique fixed point in $u_h^\varepsilon \in B_{p,h}(\rho_1)$, which is a unique solution of (27) in $B_{p,h}(\rho_1)$.

The Assertion (41) follows immediately from the fact that $u_h^\varepsilon \in B_{p,h}(\rho_1)$ and the following estimate (cf. [3])

$$\| u^\varepsilon - I_h^r u^\varepsilon \|_{W^{1,p}} \le C_6 h^r \| u^\varepsilon \|_{W^{r+1,p}}$$

for some constant $C_6 = C_6(\varepsilon) > 0$. The proof is complete. □

3.2 Error estimates in L^p-norm

In this subsection, we shall derive an error estimate for the finite element method (27) in L^p-norm using the error estimates derived in the previous subsection. Our main idea

is to use a duality argument on the linearized operator $\mathcal{L}_{u^\varepsilon}$ to handle the nonlinearity contributed by the right-hand side of Eq. (12).

The following is the second main theorem of this paper.

Theorem 5 *Let u^ε and u_h^ε denote the solutions of (12)–(14) and (27), respectively. Let h_0, h_1, and h_2 be same as in Theorem 4, then for $h \le \min\{h_0, h_1, h_2\}$, there holds for $p \in (\frac{d}{r}, \infty)$, and some $C_7 = C_7(\varepsilon) > 0$,*

$$\| u^\varepsilon - u_h^\varepsilon \|_{L^p} \le C_7 \left(h^{r+1} \| u^\varepsilon \|_{W^{r+1,p}} + h^{2r} \| u^\varepsilon \|^2_{W^{r+1,2p}} \right). \tag{43}$$

Proof Subtracting (27) from (15) yields the error equation

$$\begin{aligned} &\int_{\Omega_L} \left\{ \frac{\nabla u^\varepsilon}{|\nabla u^\varepsilon|_\varepsilon} - \frac{\nabla u_h^\varepsilon}{|\nabla u_h^\varepsilon|_\varepsilon} \right\} \cdot \nabla \varphi_h \, dx \\ &\qquad + \int_{\Omega_L} \left\{ |\nabla u^\varepsilon|_\varepsilon - |\nabla u_h^\varepsilon|_\varepsilon \right\} \varphi_h \, dx = 0 \quad \forall \varphi_h \in V_r^{h,0}. \end{aligned} \tag{44}$$

Using the Mean Value Theorem we get

$$\int_{\Omega_L} A_h^\varepsilon \nabla(u^\varepsilon - u_h^\varepsilon) \cdot \nabla \varphi_h \, dx + \int_{\Omega_L} a_h^\varepsilon \cdot \nabla(u^\varepsilon - u_h^\varepsilon) \varphi_h \, dx = 0, \tag{45}$$

where

$$\begin{aligned} A_h^\varepsilon : &= = \int_0^1 D^2 f_\varepsilon \left(\nabla u^\varepsilon + t \nabla (u_h^\varepsilon - u^\varepsilon) \right) dt, \\ a_h^\varepsilon : &= \int_0^1 D f_\varepsilon \left(\nabla u^\varepsilon + t \nabla (u_h^\varepsilon - u^\varepsilon) \right) dt. \end{aligned}$$

Again, we abuse the notation A_h^ε and a_h^ε.

Let $e_h^\varepsilon := u^\varepsilon - u_h^\varepsilon$, it follows from Lemma 1 that there exists a unique $\varphi \in W^{2,p'}(\Omega_L) \cap W_0^{1,p'}(\Omega_L)$ (recall that $\frac{1}{p} + \frac{1}{p'} = 1$) such that

$$\begin{aligned} 2\mathcal{L}^*_{u^\varepsilon}(\varphi) &= |e_h^\varepsilon|^{p-1} \mathrm{sign}(e_h^\varepsilon) \quad \text{in } \Omega_L, \\ \varphi &= 0 \quad \text{on } \partial\Omega_L, \end{aligned}$$

and

$$\| \varphi \|_{W^{2,p'}} \le C_0 \| |e_h^\varepsilon|^{p-1} \mathrm{sign}(e_h^\varepsilon) \|_{L^{p'}} \le C_0 \| e_h^\varepsilon| \|^{p-1}_{L^p}. \tag{46}$$

Testing the equation with e_h^ε and using (45) with $\varphi_h = I_h^r \varphi$ yield

$$\begin{aligned}
\| e_h^\varepsilon \|_{L^p}^p &= \int_{\Omega_L} \left\{ D^2 f_\varepsilon(\nabla u^\varepsilon) \nabla e_h^\varepsilon \cdot \nabla \varphi + D f_\varepsilon(\nabla u^\varepsilon) \cdot \nabla e_h^\varepsilon \, \varphi \right\} dx \\
&= \int_{\Omega_L} D^2 f_\varepsilon(\nabla u^\varepsilon) \nabla e_h^\varepsilon \cdot \nabla (\varphi - I_h^r \varphi) \, dx \\
&\quad + \int_{\Omega_L} D f_\varepsilon(\nabla u^\varepsilon) \cdot \nabla e_h^\varepsilon \, (\varphi - I_h^r \varphi) \, dx \\
&\quad + \int_{\Omega_L} \left[D^2 f_\varepsilon(\nabla u^\varepsilon) - A_h^\varepsilon \right] \nabla e_h^\varepsilon \cdot \nabla I_h^r \varphi \, dx \\
&\quad + \int_{\Omega_L} \left[D f_\varepsilon(\nabla u^\varepsilon) - a_h^\varepsilon \right] \cdot \nabla e_h^\varepsilon \, I_h^r \varphi \, dx
\end{aligned} \tag{47}$$

Here we have used the fact that $D^2 f(z)$ is a symmetric matrix to get the first equality. We now bound the first two terms on the right-hand side of (47) as follows

$$\begin{aligned}
&\left| \int_{\Omega_L} D^2 f_\varepsilon(\nabla u^\varepsilon) \nabla e_h^\varepsilon \cdot \nabla (\varphi - I_h^r \varphi) \, dx \right| \qquad (48) \\
&\leq 2\varepsilon^{-1} \| \nabla e_h^\varepsilon \|_{L^p} \| \nabla (\varphi - I_h^r \varphi) \|_{L^{p'}} \leq C \varepsilon^{-1} h \| \nabla e_h^\varepsilon \|_{L^p} \| \varphi \|_{W^{2,p'}}, \\
&\left| \int_{\Omega_L} D f_\varepsilon(\nabla u^\varepsilon) \cdot \nabla e_h^\varepsilon \, (\varphi - I_h^r \varphi) \, dx \right| \qquad (49) \\
&\leq \| \nabla e_h^\varepsilon \|_{L^p} \| \varphi - I_h^r \varphi \|_{L^{p'}} \leq C h^2 \| \nabla e_h^\varepsilon \|_{L^p} \| \varphi \|_{W^{2,p'}}.
\end{aligned}$$

It follows from (39) and the Mean Value Theorem that

$$\left| D^2 f_\varepsilon(\nabla u^\varepsilon) - A_h^\varepsilon \right| \leq 9\varepsilon^{-2} |\nabla e_h^\varepsilon|, \quad \left| D f_\varepsilon(\nabla u^\varepsilon) - a_h^\varepsilon \right| \leq 2\varepsilon^{-1} |\nabla e_h^\varepsilon|.$$

Also, notice that A_h^ε and a_h^ε are controlled by the same upper bounds as $D^2 f_\varepsilon(\nabla u^\varepsilon)$ and $D f_\varepsilon(\nabla u^\varepsilon)$ are, respectively, that is

$$\left| (A_h^\varepsilon)_{ij} \right| \leq 2\varepsilon^{-1} \qquad \left| (a_h^\varepsilon)_i \right| \leq 1 \qquad \text{for } 1 \leq i, j \leq d,$$

Using approximation properties of I_h^r and the Poincaré inequality we get

$$\begin{aligned}
&\left| \int_{\Omega_L} \left[D^2 f_\varepsilon(\nabla u^\varepsilon) - A_h^\varepsilon \right] \nabla e_h^\varepsilon \cdot \nabla I_h^r \varphi \, dx \right| \\
&\quad \le \int_{\Omega_L} \left| D^2 f_\varepsilon(\nabla u^\varepsilon) - A_h^\varepsilon \right| |\nabla e_h^\varepsilon| \, |\nabla I_h^r \varphi| \, dx \\
&\quad \le 9\varepsilon^{-2} \int_{\Omega_L} |\nabla e_h^\varepsilon|^2 |\nabla I_h^r \varphi| \, dx \le C\varepsilon^{-2} \| \nabla e_h^\varepsilon \|_{L^{2p}}^2 \| \varphi \|_{W^{2,p'}}, \qquad (50)
\end{aligned}$$

$$\begin{aligned}
&\left| \int_{\Omega_L} \left[Df_\varepsilon(\nabla u^\varepsilon) - a_h^\varepsilon \right] \cdot \nabla e_h^\varepsilon \, I_h^r \varphi \, dx \right| \\
&\quad \le 2\varepsilon^{-1} \int_{\Omega_L} |\nabla e_h^\varepsilon|^2 \, |I_h^r \varphi| \, dx \le C\varepsilon^{-1} \| \nabla e_h^\varepsilon \|_{L^{2p}}^2 \| \varphi \|_{W^{2,p'}}. \qquad (51)
\end{aligned}$$

Substituting (48), (49), (50), (51), and (46) into (47) yields

$$\| e_h^\varepsilon \|_{L^p} \le CC_0\varepsilon^{-2} \left(h \| \nabla e_h^\varepsilon \|_{L^p} + \| \nabla e_h^\varepsilon \|_{L^{2p}}^2 \right),$$

which together with Theorem 4 lead to the desired estimate. The proof is complete. □

Remark 6 We note that the proof of Theorem 5 can not be carried over to the case $p = \infty$ because the estimate (46) does not hold for $p' = 1$ in general. On the other hand, one can get an L^∞-norm error estimate by using a unique continuation idea as utilized in [9]. However, the explicit dependence of the error constant on the parameter ε will be lost in the derivation.

4 Passing to the limit as $\varepsilon \to 0$

The goal of this section is to address convergence of the finite element solution u_h^ε to the solution of (8)–(10). It turns out that the convergence actually is a simple corollary of the error estimate (43) and the convergence (16), which gives the third main theorem of this paper.

Theorem 6 *Let u^0 and u_h^ε denote the solution of (8)–(10) and (27), respectively. Then, there exists a constant $C_8 = C_8(\varepsilon) > 0$, such that for $h \le C_8^{-1}(\varepsilon)$ there holds that*

$$\lim_{\varepsilon \to 0} \| u^0 - u_h^\varepsilon \|_{L^\infty_{loc}} = 0. \qquad (52)$$

Proof For any compact subset $A \subset \Omega$, there exists $\varepsilon_0 > 0$ such that $A \subset \Omega_L$ for $\varepsilon \in (0, \varepsilon_0)$. By (16) we know that u^ε converges to u^0 uniformly on A.

Using the error bound (43), the inverse inequality bounding the L^∞-norm in terms of the L^p-norm, the approximation properties of the interpolation operator I_h^r (cf. [7]), and the fact that $2r \geq r+1$ we get for $0 < \varepsilon < \varepsilon_0$

$$\begin{aligned}
&\| u^\varepsilon - u_h^\varepsilon \|_{L^\infty(A)} \leq \| u^\varepsilon - u_h^\varepsilon \|_{L^\infty(\Omega_L)} \\
&\leq \| u^\varepsilon - I_h^r u^\varepsilon \|_{L^\infty(\Omega_L)} + \| I_h^r u^\varepsilon - u_h^\varepsilon \|_{L^\infty(\Omega_L)} \\
&\leq C\, h^{r+1} \| u^\varepsilon \|_{W^{r+1,\infty}(\Omega_L)} + C\, h^{-\frac{d}{p}} \| I_h^r u^\varepsilon - u_h^\varepsilon \|_{L^p(\Omega_L)} \\
&\leq C\, h^{r+1} \| u^\varepsilon \|_{W^{r+1,\infty}(\Omega_L)} \\
&+ C\, h^{-\frac{d}{p}} \left\{ \| I_h^r u^\varepsilon - u^\varepsilon \|_{L^p(\Omega_L)} + \| u^\varepsilon - u_h^\varepsilon \|_{L^p(\Omega_L)} \right\} \\
&\leq C\, h^{r+1} \| u^\varepsilon \|_{W^{r+1,\infty}(\Omega_L)} + h^{r+1-\frac{d}{p}} \left\{ \| u^\varepsilon \|_{W^{r+1,p}(\Omega_L)} + C_7 \right\}.
\end{aligned}$$

Since $r+1 > \frac{d}{p}$ for $p \geq 2$ and $r \geq 1$, there exists $C_8 = C_8(\varepsilon) > 0$, such that $h^{r+1-\frac{d}{p}} \{ \| u^\varepsilon \|_{W^{r+1,p}} + C_7 \}$ tends to zero for $h \leq C_8^{-1}$, and $\varepsilon \to 0$.

Finally, (52) follows from the following triangle inequality

$$\| u^0 - u_h^\varepsilon \|_{L^\infty(A)} \leq \| u^0 - u^\varepsilon \|_{L^\infty(A)} + \| u^\varepsilon - u_h^\varepsilon \|_{L^\infty(A)} \to 0$$

as $\varepsilon \to 0$. The proof is complete. □

Remark 7 Since the convergence (16) does not give a rate of convergence for $\| u^0 - u^\varepsilon \|_{L^\infty_{\text{loc}}}$, hence, the above proof does not provide any rate of convergence for $\| u^0 - u_h^\varepsilon \|_{L^\infty_{\text{loc}}}$ either. It may be possible to derive a rate convergence by directly examining the error $u^0 - u_h^\varepsilon$, in particular, in a weaker norm.

5 Numerical experiments and rates of convergence

In this section we first provide several 2-D numerical experiments to show the efficiency of the finite element method developed in the previous section, and numerically to validate the "jumping out" phenomenon of the weak solution of the inverse mean curvature flow, which corresponds to the discontinuity in t of the function $t = u^0(x)$, where u^0 is the solution to (8)–(10). We numerically study the "best" choice of the mesh size $h = h(\varepsilon)$, which also alludes dependence of C_7 on ε^{-1} in (43), and rates of convergence for both, $u^0 - u_h^\varepsilon$ and $u^0 - u^\varepsilon$, in terms of powers of ε. We note that no rate of convergence for $u^0 - u^\varepsilon$ was given in [17]. Moreover, we present a numerical study of the rates of convergence for Moser's approach (The inverse mean curvature flow and p-harmonic functions. preprint U Bath, 2005) for approximating the inverse mean curvature flow via p-harmonic functions (see Remark 3).

5.1 Validation of the "jumping out" phenomenon

All our numerical experiments given in this subsection are done on the domain $\Omega_L := B_{10}(0) \backslash E_0$ for different choices of the initial domain E_0 or the initial curve $\Gamma_0 = \partial E_0$.

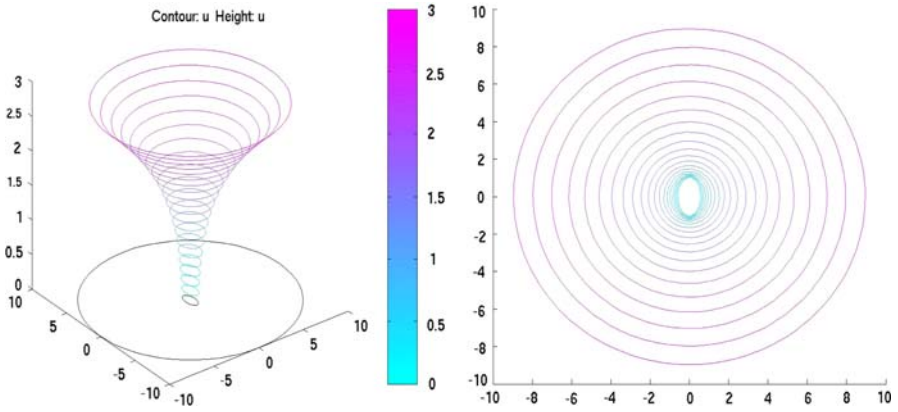

Fig. 1 Contours of computed solution u_h^ε of Test 1

Also all our numerical experiments are done using regularization parameter $\varepsilon = 10^{-2}$, mesh parameter $h = 10^{-4}$, and linear finite element. As pointed out in (b) of Remark 2, choosing the "correct" Dirichlet boundary value L is very tricky for designing a numerical test problem, since (12)–(14) may have no solution if L is chosen too large. This theoretical prediction of [17] is indeed observed in our numerical experiments. In all our numerical experiments we find out the "correct" L simply by trial and error.

Test 1: In this experiment, we choose $L = 3$ and the starting curve is the ellipse centered at the origin with long radius 1 and short radius 0.5. As expected, the inverse mean curvature flow Γ_t is a family of expanding ellipses at the very beginning of the evolution, and quickly rounds to a circle. From there the flow becomes a family of expanding circles as seen in Tests 1 and 2.

Figure 1 shows 20 contour plots of the computed solution u_h^ε, the graph on left shows both the contours and the heights of u_h^ε values, while the graph on right only shows the contours of u_h^ε. In this test, the "magic" number for L is around 3, we find numerically that the finite element equation (27) has no solution when $L \geq 3.1$.

The goal of the next experiment is to show the ability of the generalized inverse mean curvature flow to evolve curves with *flat* parts. We remark that since the mean curvature equal zero on the flat parts, the classical inverse mean curvature flow (1) is not defined for such curves.

Test 2: In this experiment, we choose $L = 4$ and E_0 is the unit square centered at the origin. Hence, our starting curve is $\Gamma_0 = \{(x_1, x_2);\ x_1 = \pm 0.5, -0.5 \leq x_2 \leq 0.5 \text{ and } x_2 = \pm 0.5, -0.5 \leq x_1 \leq 0.5\}$. As expected, the inverse mean curvature flow Γ_t is a family of expanding squares at the very beginning of the evolution, and quickly rounds to a circle. From there the flow becomes a family of expanding circles as seen in Tests 1 and 2.

Figure 2 shows 20 contour plots of the computed solution u_h^ε, the graph on the left shows both, the contours and the heights of u_h^ε values, while the graph on right only shows the contours of u_h^ε. The "magic" number for L in this test is around 4, we find numerically that the finite element equation (27) has no solution when $L \geq 4.1$.

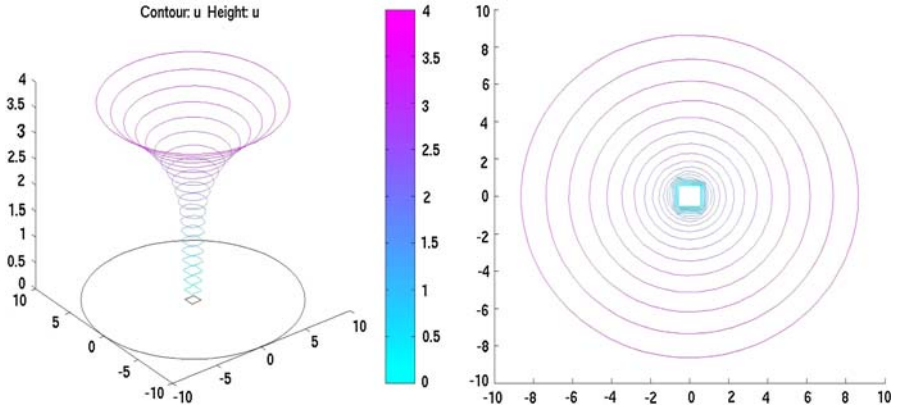

Fig. 2 Contours of computed solution u_h^ε of Test 2

From the definition it is easy to see that the (level set) weak formulation of the inverse mean curvature flow does not require the starting hypersurface to be connected. In fact, it does not matter if the starting hypersurface has two or more disjoint components. The goal of the next experiment is to show the ability of the generalized inverse mean curvature flow to evolve two disjoint circles, and to observe the "jumping out" phenomenon of the the weak solution of the flow, which corresponds to discontinuity of the function $t = u^0(x)$ in t.

Test 3: In this experiment we take $L = 4$, and Γ_0 are two disjoint unit circles centered at $(-2, 0)$ and $(2, 0)$ (hence, separated by a distance of two units). The classical solution for the inverse mean curvature flow exists up to the point $t = t_{\text{touch}}$ when the two expanding circles would touch. However, the weak formulation jumps to the minimizing hull at $t = t_{\text{jump}}$ long before $t = t_{\text{touch}}$ is reached. Notice that a catenoid is formed to bridge the two circles at $t = t_{\text{jump}}$, from that point on the connected curve becomes round and round, and quickly evolves into a bigger circle. Afterward, the flow becomes a family of expanding circles as seen in Tests 1 and 2.

Figure 3 shows 20 contour plots of the computed solution u_h^ε, which captures all the actions described above. The graph on left shows both the contours and the heights of u_h^ε values, while the graph on right only shows the contours of u_h^ε. Again, the "magic" number for L in this test is around 4, we find numerically that the finite element equation (27) has no solution when $L \geq 4.1$.

Test 4: The only difference between this experiment and the previous experiment is that the starting curve Γ_0 is changed to two disjoint circles of radius 2 centered at $(-3, 0)$ and $(3, 0)$, respectively. So the two larger circles are still separated by a distance of two units. The computed solution u_h^ε is given in Fig. 4. The simulation shows that because the two starting circles are so close to each other (relative to their sizes), they jump to form a connected curve in almost no time under the generalized inverse mean curvature flow. Also, we estimate that the "magic" number for L in this test is around 4.

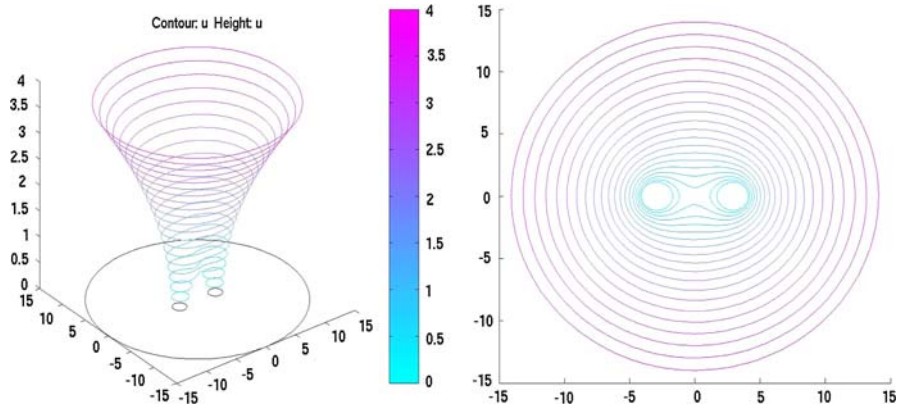

Fig. 3 Contours of computed solution u_h^ε of Test 3

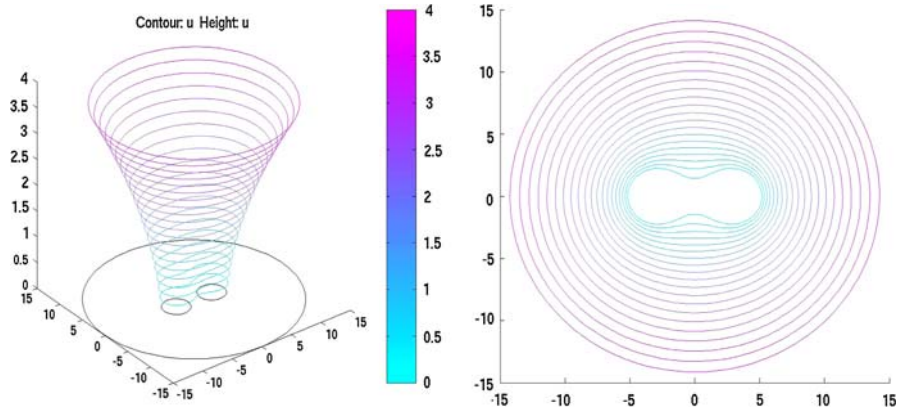

Fig. 4 Contours of computed solution u_h^ε of Test 4

5.2 Rates of convergence for $u^0 - u_h^\varepsilon$ and $u^0 - u^\varepsilon$

It is interesting and important to know how fast u^ε converges to u^0 as $\varepsilon \to 0$ and how fast u_h^ε converges to u^0 as $\varepsilon \to 0$, with $h \le C_8(\varepsilon)$. Theoretically, it is very difficult to estimate these rates of convergence, if it is possible. In this subsection, we shall address these issues numerically, that is, to estimate these rates of convergence by numerical tests and to make predictions based on the numerical results.

Test 5: In this test, we examine the rate of convergence of the error $\|u^\varepsilon - u_h^\varepsilon\|_{L^2}$ for a fixed ε in the case of linear finite element. We solve the following nonhomogeneous equation

$$-\mathrm{div}\left(\frac{\nabla u^\epsilon}{\sqrt{|\nabla u^\epsilon|^2+\epsilon^2}}\right)+\sqrt{|\nabla u^\epsilon|^2+\epsilon^2}=g^\epsilon,$$

Table 1 Change of $\|e_h^\varepsilon\|_{L^2}$ with respect to h and ε ($e_h^\varepsilon := u^\varepsilon - u_h^\varepsilon$)

# of elements n	h	$\|e_h^\varepsilon\|_{L^2}$	$\|e_h^\varepsilon\|_{L^2}/h^2$
$\varepsilon = 0.1$			
5	0.2	0.013372718	0.334317962
10	0.1	0.003338604	0.33386045
20	0.05	0.000834378	0.333751093
40	0.025	0.000208577	0.333722874
80	0.0125	5.21431E−05	0.333715909
160	0.00625	1.30358E−05	0.333715614
$\varepsilon = 0.01$			
5	0.2	0.013372307	0.33430768
10	0.1	0.003338495	0.333849517
20	0.05	0.00083435	0.333740114
40	0.025	0.00020857	0.33371202
80	0.0125	5.21415E−05	0.33370559
160	0.00625	1.30354E−05	0.333707366
$\varepsilon = 0.001$			
5	0.2	0.013372303	0.334307587
10	0.1	0.003338495	0.333849517
20	0.05	0.00083435	0.333739995
40	0.025	0.00020857	0.333711866
80	0.0125	5.21415E−05	0.333705353
160	0.00625	1.30354E−05	0.333706679
$\varepsilon = 0.0001$			
5	0.2	0.013372303	0.334307587
10	0.1	0.003338495	0.333849517
20	0.05	0.00083435	0.333739995
40	0.025	0.00020857	0.333711866
80	0.0125	5.21415E−05	0.333705292
160	0.00625	1.30354E−05	0.333706679

on the domain $\Omega = \{(x, y);\ 1 < x < 2,\ 1 < y < 2\}$, where

$$g^\epsilon := \frac{-4}{\varphi^\epsilon(x, y)} + \frac{8x^2 + 8y^2}{\varphi^\epsilon(x, y)^3} + \varphi^\epsilon(x, y), \quad \varphi^\epsilon := \sqrt{4x^2 + 4y^2 + \epsilon^2}.$$

It is easy to check that $u(x, y) = x^2 + y^2$ is the unique exact solution of the above equation with matched boundary condition.

The numbers on the last column of Table 1 clearly show that $\|u^\varepsilon - u_h^\varepsilon\|_{L^2} = O(h^2)$ for each fixed ε, which is expected for the linear finite element. Moreover, this rate is robust with respect to ε since the constants do not deteriorate as ε becomes small.

Test 6: The goals of this test are: (1) to determine the rate of convergence $u^0 - u^\varepsilon$; (2) to find the "best" choice of h in terms of ε such that the global error $u^0 - u_h^\varepsilon$ is of

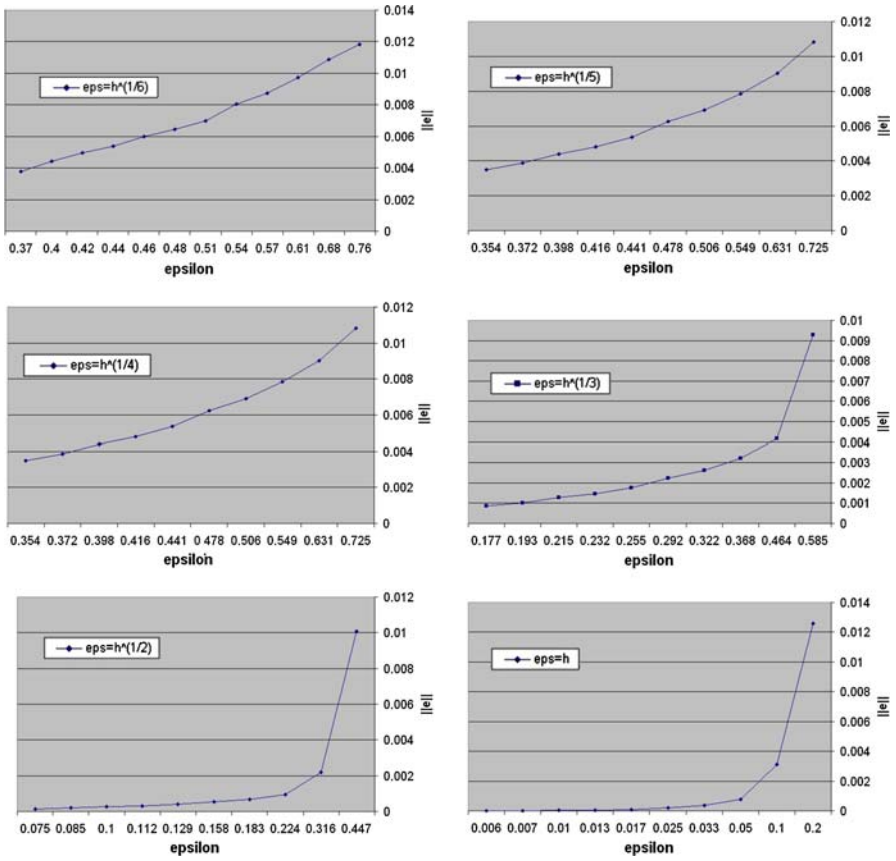

Fig. 5 Change of $\|u^0 - u_h^\varepsilon\|_{L^2}$ as a function of ε

the same convergence rate as that for $u^0 - u^\varepsilon$. Let Ω be same as in Test 5, and choose g such that $u(x, y) = x^2 + y^2$ solves

$$-\text{div}\left(\frac{\nabla u}{|\nabla u|}\right) + |\nabla u| = g.$$

Figure 5 displays the error $\|u^0 - u_h^\epsilon\|_{L^2}$ using various parameter laws $h = O(\varepsilon^\alpha)$. The aim here is to determine the rates of convergence for $\|u^0 - u_h^\epsilon\|_{L^2}$ and $\|u^0 - u^\epsilon\|_{L^2}$ in terms of ε. From all graphs we see that the error $\|u^0 - u_h^\epsilon\|_{L^2}$ becomes a *linear* function of ε as soon as ε is less than a threshold value ε_0. As expected, this threshold value ε_0 depends on the choice of $h = O(\varepsilon^\alpha)$. Since for large α (such as $\alpha \geq 4$), h is extremely small, so is error $\|u^\varepsilon - u_h^\epsilon\|_{L^2}$. Hence, $\|u^0 - u^\epsilon\|_{L^2} \approx \|u^0 - u_h^\epsilon\|_{L^2} = O(\varepsilon)$ for $\varepsilon \in (0, \varepsilon_0)$. Based on this heuristic argument, we predict that $\|u^0 - u^\epsilon\|_{L^2} = O(\varepsilon)$. Moreover, since the threshold value ε_0 is reasonably large when $h = \varepsilon^2$, we conjecture that $h = O(\varepsilon^2)$ is the "best" choice for practical simulations.

5.3 Rates of convergence for $u^0 - u^{\varepsilon}_{p,h}$ and $u^0 - u_p$

In this subsection, we present some numerical tests for Moser's approach (The inverse mean curvature flow and p-harmonic functions. preprint U Bath, 2005) which approximates the inverse mean curvature flow via p-harmonic functions (cf. Remark 3). To the end, we first approximate the degenerate exterior domain problem

$$\begin{aligned} 2\mathrm{div}\left(|\nabla v_p|^{p-2}\nabla v_p\right) &= \frac{g_p v_p^{p-1}}{(p-1)^{p-1}} \quad \text{in } \Omega, \\ v_p &= 1 \quad \text{on } \partial\Omega^-, \\ v_p &\to \infty \quad \text{as } |x| \to \infty, \end{aligned}$$

by the following regularized problem

$$2\mathrm{div}\left((|\nabla v_p^{\epsilon}|^2 + \epsilon^2)^{\frac{p-2}{2}}\nabla v_p^{\epsilon}\right) = \frac{g_p v_p^{p-1}}{(p-1)^{p-1}} \quad \text{in } \Omega_L, \tag{53}$$

$$v_p^{\epsilon} = 1 \quad \text{on } \partial\Omega_L^-, \tag{54}$$

$$v_p^{\epsilon} = L \quad \text{on } \partial\Omega_L^+, \tag{55}$$

where $L >> 1$. Here we have used the fact that if u_p solves

$$-\mathrm{div}\left(|\nabla u_p|^{p-2}\nabla u_p\right) + |\nabla u_p|^p = g_p,$$

then $v_p = e^{-\frac{u_p}{p-1}}$ solves

$$\mathrm{div}\left(|\nabla v_p|^{p-2}\nabla v_p\right) = \frac{g_p v_p^{p-1}}{(p-1)^{p-1}}.$$

Let $\Omega = \{(x, y);\ 0 < x < 1, 0 < y < 1\}$, we choose an appropriate function g_p such that $u(x, y) = x^2 + y^2$ solves

$$-\mathrm{div}\left(|\nabla u_p|^{p-2}\nabla u_p\right) + |\nabla u_p|^p = g_p.$$

In the following we shall compute the finite element solution $v^{\varepsilon}_{p,h}$ for (53)–(55), and then define $u^{\varepsilon}_{p,h} = (1-p)\log(v^{\varepsilon}_{p,h})$.

Figure 6 displays the error $\|u_p - u^{\epsilon}_{p,h}\|_{L^2}$ for $p = 1.5$ fixed while varying the mesh size h and parameter ε. The aim here is to determine the rates of convergence for $\|u_p - u^{\epsilon}_{p,h}\|_{L^2}$ and $\|u_p - u^{\epsilon}_{p}\|_{L^2}$ in terms ε. From all graphs we see that the error $\|u_p - u^{\epsilon}_{p,h}\|_{L^2}$ becomes a *linear* function of ε as soon as ε is less than a threshold value ε_1. As expected, this threshold value ε_1 depends on the choice of $h = O(\varepsilon^{\alpha})$. Since for large α (such as $\alpha \geq 4$), h is extremely small, so is error $\|u^{\varepsilon}_{p} - u^{\epsilon}_{p,h}\|_{L^2}$. Hence, $\|u_p - u^{\epsilon}_{p}\|_{L^2} \approx \|u_p - u^{\epsilon}_{p,h}\|_{L^2} = O(\varepsilon)$ for $\varepsilon \in (0, \varepsilon_1)$. Based on this heuristic

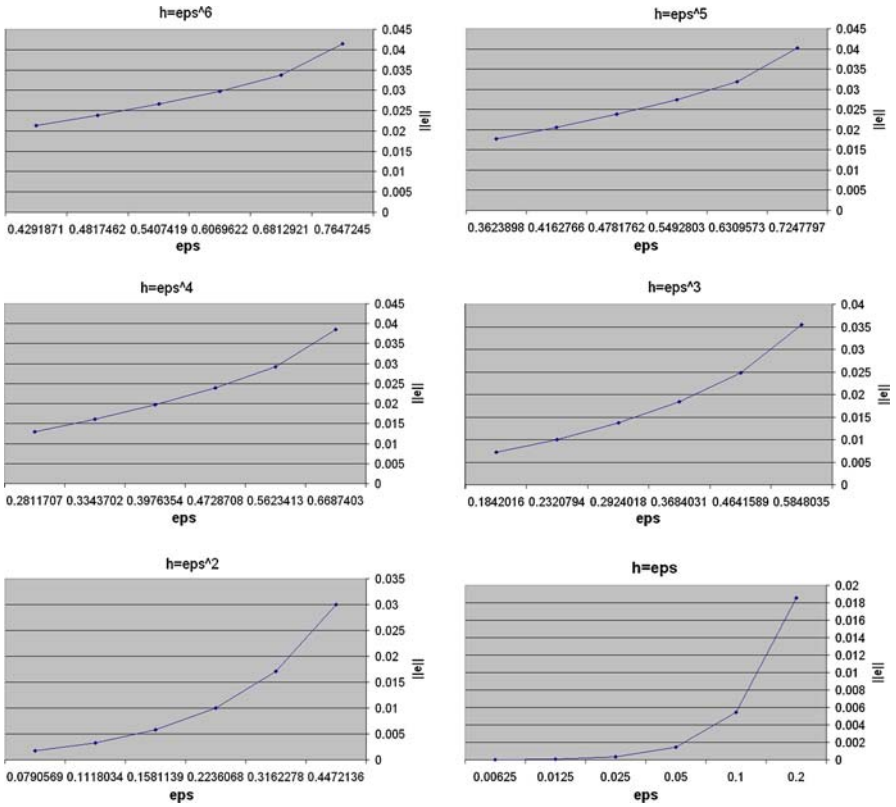

Fig. 6 Error $\|u_p - u^{\varepsilon}_{p,h}\|_{L^2}$ as a function of ε

argument, we predict that $\|u_p - u^{\epsilon}_p\|_{L^2} = O(\varepsilon)$. Moreover, since the threshold value ε_1 is reasonably large when $h = \varepsilon^2$, we conjecture that $h = O(\varepsilon^2)$ is the "best" choice for practical simulations.

Test 7: The goal of this test is to determine the rate of convergence of $\|u^0 - u^{\varepsilon}_{p,h}\|_{L^2}$ and $\|u^0 - u_p\|_{L^2}$ in terms of $p - 1$. To the end, we fix $h = \varepsilon$ in all simulations. Let Ω be the same as in Test 6, and choose g to be an appropriate function such that $u(x, y) = x^2 + y^2$ solves

$$-\mathrm{div}\left(\frac{\nabla u}{|\nabla u|}\right) + |\nabla u| = g.$$

Figure 7 displays the error $\|u^0 - u^{\varepsilon}_{p,h}\|_{L^2}$ as a function of $(p-1)$ with fixed parameter law $\varepsilon = h$ with various choices of h. We observe that the error $\|u^0 - u^{\varepsilon}_{p,h}\|_{L^2}$ becomes a linear function of $(p - 1)$ when $p - 1$ is less than a threshold value σ_0, that is, when $p < 1 + \sigma_0$. We then predict that $\|u^0 - u^{\varepsilon}_{p,h}\|_{L^2} = O(p - 1)$. Since for very small $\varepsilon = h$, $\|u^0 - u_p\|_{L^2} \approx \|u^0 - u^{\varepsilon}_{p,h}\|_{L^2} = O(p - 1)$, so we also predict that $\|u^0 - u_p\|_{L^2} = O(p - 1)$ as p tends to 1.

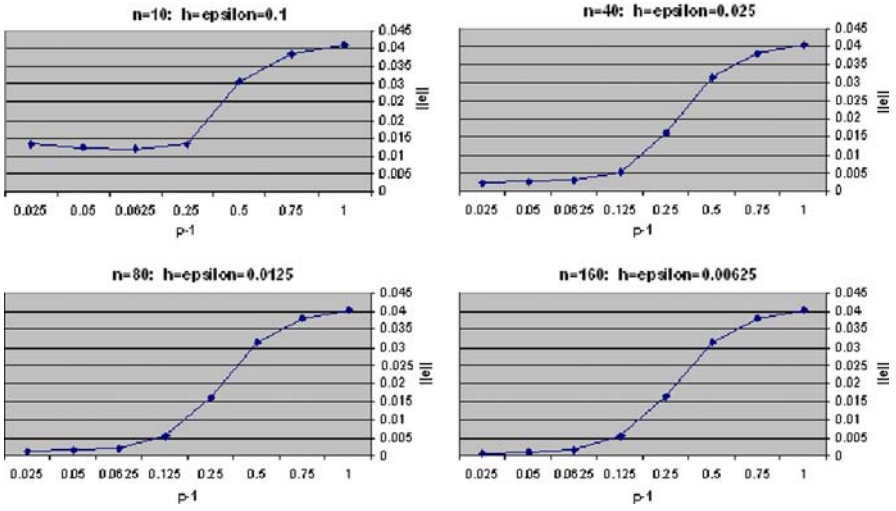

Fig. 7 Error $\|u^0 - u^{\varepsilon}_{p,h}\|_{L^2}$ in $p-1$ and ε with $h = \varepsilon$

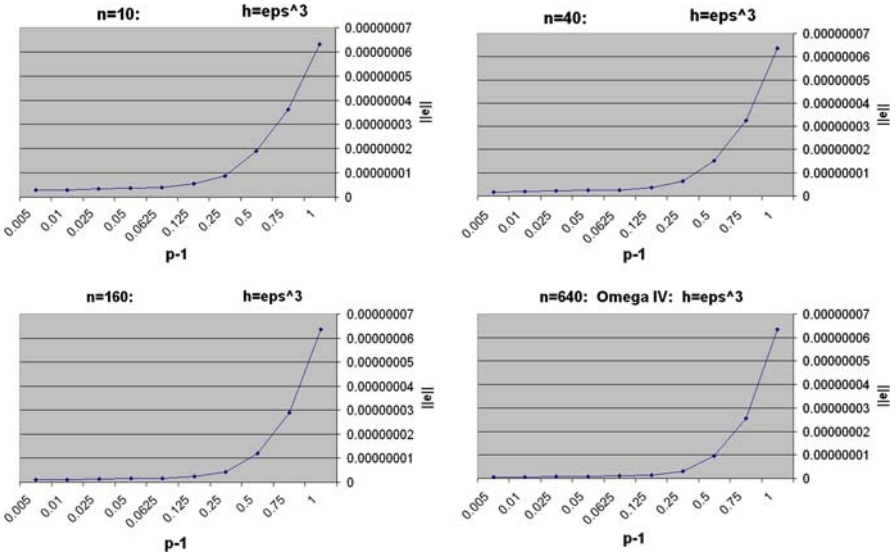

Fig. 8 Error $\|u^0 - u^{\varepsilon}_{p,h}\|_{L^2(\Omega_1)}$ as a function of $(p-1)$

Test 8: To confirm the convergence rate prediction of Test 7, we perform some more simulations using extremely high resolutions which correspond to choices of extremely small parameter ε and h. To the end, we need to zoom in at a small part of the computational domain otherwise the amount of computations is too large to be done on a desktop computer. Set $\Omega_1 = \{(x, y)|0 < x < 0.001, 0 < y < 0.001\}$, let u and g be same as in Test 7. Figure 8 displays the error $\|u^0 - u^{\varepsilon}_{p,h}\|_{L^2(\Omega_1)}$ as a function

of $(p-1)$. The graphs clearly show the asymptotic rate $\|u^0 - u^{\varepsilon}_{p,h}\|_{L^2(\Omega_1)} = O(p-1)$, hence $\|u^0 - u_p\|_{L^2(\Omega_1)} = O(p-1)$, as p tends to 1.

Acknowledgments The work of the first two authors were partially supported by the NSF grant DMS-0410266.

References

1. Adams, R.A.: Sobolev Spaces. Academic, New York (1975)
2. Bray, H.: Proof of the Riemannian Penrose inequality using the positive mass theorem. J. Diff. Geom. **59**, 177–267 (2001)
3. Brenner, S.C., Scott, L.R.: The Mathematical Theory of Finite Element Methods. Springer, Heidelberg (1994)
4. Carroll, S.M.: Spacetime and Geometry—An Introduction to General Relativity. Addison Wesley, Reading (2003)
5. Crandall, M.G., Ishii, H., Lions, P.L.: User's guide to viscosity solutions of second order partial differential equations. Bull. Am. Math. Soc. (N.S.) **27**, 1–67 (1992)
6. Chen, Y.-G., Giga, Y., Goto, S.: Uniqueness and existence of viscosity solutions of generalized mean curvature flow equations. J. Diff. Geom. **33**, 749–786 (1991)
7. Ciarlet, P.G.: Basic error estimates for elliptic problems, in Handbook of Numerical Analysis, I, pp 17–351. North-Holland, Amsterdam (1991)
8. Crouzeix, M., Thomee, V.: The stability in L^p and W^1_p of the $L2$-projection onto Finite element Function Spaces. Math. Comp. **48**, 521–532 (1987)
9. Dobrowolski, M., Rannacher, R.: Finite element methods for nonlinear elliptic systems of second order. Math. Nachr. **94**, 155–172 (1980)
10. Douglas, J. Jr, Santos, E., Sheen, D., Schreyer, L.: Frequency domain treatment of one-dimensional scalar waves. Math. Models Methods Appl.-Sci. **3**, 171–194 (1993)
11. Evans, L.C., Spruck, J.: Motion of level sets by mean curvature. I. J. Diff. Geom. **33**, 635–681 (1991)
12. Geroch, R.: Energy extraction. Ann. New York Acad. Sci. **224**, 108–117 (1973)
13. Feng, X., Prohl, A.: Analysis of total variation flow and its finite element approximations. Math. Model. Numer. Anal. **37**, 533–556 (2003)
14. Feng, X., Oehsen, M. von , Prohl, A.: Rate of convergence of regularization procedures and finite element approximations for the total variation flow. Numer. Math. **100**, 441–456 (2005)
15. Gilbarg, D., Trudinger, N.: Elliptic Partial Differential Equations of Second Order, 3rd edn. Springer, Heidelberg (2001)
16. Girault, V., Raviart, P.A.: Finite element methods for Navier–Stokes equations. Springer, Heidelberg (1986)
17. Huisken, G., Ilmanen, T.: The inverse mean curvature flow and the Riemannian Penrose Inequality. J. Diff. Geom. **59**, 353–437 (2001)
18. Huisken, G., Ilmanen, T.: A note on the inverse mean curvature flow. In: Proceedings of Workshop at Saitama University (September 1997), March 1998
19. Holder, M.: Contracting spacelike hypersurfaces by their inverse mean curvature. J. Austral. Math. Soc. Ser. A. **68**, 121–133 (2000)
20. Jang, P.S.: On positive energy conjecture. J. Math. Phys. **17**, 141–145 (1976)
21. Jang, P.S.: On the positivity of the mass for black hole space-times. Commun. Math. Phys. **69**, 257–266 (1979)
22. Jang, P.S., Wald, R.M.: The positive energy conjecture and the cosmic censorship hypothesis. J. Math. Phys. **18**, 41–44 (1977)
23. Ladyženskaja, O.A., Uarlceva, N.N.: Linear and Quasilinear Elliptic Equations. Academic, New York (1967)
24. Osher, S., Fedkiw, R.: Level Set Methods and Dynamic Implicit Surfaces. Springer, New York (2003)
25. Osher, S., Sethian, J.A.: Fronts propagating with curvature-dependent speed: algorithms based on Hamilton-Jacobi formulations. J. Comput. Phys. **79**, 12–49 (1988)
26. Pasch, E.: Numerische Verfahren zur Berechnung von Krümmungsflüssen. PhD Dissertation, Universität Tübingen (1998)

27. Pousin, J., Rappaz, J.: Consistency, stability, a priori and a posteriori errors for Petrov-Galerkin methods applied to nonlinear problems. Numer. Math. **69**, 213–231 (1994)
28. Simader, C.G.: On Dirichlet's Boundary Value Problem. Lecture Notes in Mathematics, No. 268. Springer, Heidelberg (1972)
29. Schoen, R., Yau, S.-T.: On the proof of the positive mass conjecture in general relativity. Comm. Math. Phys. **65**, 45–76 (1979)
30. Schoen, R., Yau, S.-T.: Proof of the positive mass theorem II. Commun. Math. Phys. **79**, 231–260 (1981)
31. Schatz, A.: An observation concerning Ritz–Galerkin methods with indefinite bilinear forms. Math. Comp. **28**, 959–962 (1974)